Elsevier Editorial System(tm) for Construction & Building Materials
Manuscript Draft

Manuscript Number: CONBUILDMAT-D-14-01827R1

Title: Mechanical and hydration properties of ground granulated blastfurnace slag pastes activated with MgO-CaO mixtures

Article Type: Research Paper

Keywords: Alkali-activated slag; Reactive MgO; CaO; Hydration

Corresponding Author: Dr. Kai Gu, Ph.D.

Corresponding Author's Institution: Nanjing University

First Author: Kai Gu, Ph.D.

Order of Authors: Kai Gu, Ph.D.; Fei Jin, Ph.D.; Abir Al-Tabbaa, Ph.D.; Bin Shi, Ph.D.; Jin Liu, Ph.D.

Abstract: Since alkali-activated slag using conventional activators suffers from economical and technical problems, other alternative activators should be explored. This paper reports the results of an investigation into the activation of ground granulated blastfurnace slag by using 10% (by weight) reactive MgO, CaO and their mixtures with various ratios. The mechanical and hydration properties of pastes were examined up to 90 days. It was found that the strength of slag pastes activated with MgO-CaO mixtures decreased with the increasing ratio of MgO to CaO in the early age while a much steeper strength gain was observed in pastes with MgO/CaO higher than 19/1 after 28 days and longer. The addition of small amount of CaO in MgO can greatly accelerate the hydration of slag in the early age by increasing the pH of pore solution. However, pastes showed small difference in strength development at each period when MgO/CaO was less than 1. The main hydration products, analysed by XRD, TGA and SEM/EDS, were C-S-H and hydrotalcite-like phases. While CaO accelerated the formation of C-S-H in the early age, MgO induced more amount of hydrotalcite-like phases, which notably enhanced the strength of slag pastes with high MgO content after 28 days and longer. Calcite, portlandite and residual MgO were also observed, depending on the MgO/CaO ratio and the hydration time. This work indicated that the replacement of MgO by CaO can make the application of reactive MgO in slag activation more economical.

Mechanical and hydration properties of ground granulated blastfurnace slag pastes activated with MgO-CaO mixtures

Kai Gu[1,2,*], Fei Jin[2,*], Abir Al-Tabbaa[2], Bin Shi[1], Jin Liu[3]

[1] School of Earth Sciences and Engineering, Nanjing University,163 Xianlin Avenue, Nanjing, China, 210093

[2] Department of Engineering, University of Cambridge, Trumpington Road, Cambridge, UK, CB2 1PZ

[3] School of Earth Sciences and Engineering, Hohai University, 1 Xikang Road, Nanjing, China, 210098

*Corresponding authors: Kai Gu: gukainju@gmail.com, Fei Jin: fj232@cam.ac.uk

ABSTRACT: Since alkali-activated slag using conventional activators suffers from economical and technical problems, other alternative activators should be explored. This paper reports the results of an investigation into the activation of ground granulated blastfurnace slag by using 10% (by weight) reactive MgO, CaO and their mixtures with various ratios. The mechanical and hydration properties of pastes were examined up to 90 days. It was found that the strength of slag pastes activated with MgO-CaO mixtures decreased with the increasing ratio of MgO to CaO in the early age while a much steeper strength gain was observed in pastes with MgO/CaO higher than 19/1 after 28 days and longer. The addition of small amount of CaO in MgO can greatly accelerate the hydration of slag in the early age by increasing the pH of pore solution. However, pastes showed small difference in strength development at each period when MgO/CaO was less than 1. The main hydration products, analysed by XRD, TGA and SEM/EDS, were C-S-H and hydrotalcite-like phases. While CaO accelerated the formation of C-S-H in the early age, MgO induced more amount of hydrotalcite-like phases, which notably enhanced the strength of slag pastes with high MgO content after 28 days and longer. Calcite, portlandite and residual MgO were also observed, depending on the MgO/CaO ratio and the hydration time. This work indicated

that the replacement of MgO by CaO can make the application of reactive MgO in slag activation more economical.

Keywords: Alkali-activated slag; Reactive MgO; CaO; Hydration

1. Introduction

Climate change, attributed by large to greenhouse gas emissions, has been a major threat to human society. Among the most energy-intensive industries, the cement industry contributes ~5-8% of global man-made CO_2 emissions [1], mainly because of the direct calcination of limestone and the consumption of fossil fuels. The search for more sustainable binders has led to the development of alkali-activated cements (AACs), which utilise a large portion of supplementary cementitious materials (SCMs), such as blastfurnace slag, fly ash, metakaolin and silica fume [2,3]. The most widely used activators in AAC are sodium silicate, sodium hydroxide, sodium carbonate or a mixture of sodium-potassium hydroxide with sodium silicate-potassium silicate [1,4]. However, most of these activators do not exist naturally and they are obtained from energy intensive manufacturing processes, which expands the energy consumption associated with AAC. A comparison of the carbon dioxide equivalent (CO_2-e) emissions between alkali-activated fly ash and ordinary PC indicated that only ~9% reduction was obtained by using the former instead of ~26-80% (as previously claimed [5,6]) when considering the energy consumption associated with the manufacturing process of activators [7]. Other issues should also be carefully considered when using these conventional activators, including the fast setting time, the high drying shrinkage, the highly corrosive nature of alkali solutions, the viscosity of alkali solution and the heat released by the dissolution of the alkali compounds, especially alkali hydroxide, during preparation of the solutions [1,8–10]. In order to tackle the above mentioned technical and environmental challenges associated with the conventional alkali activators used in AAC, alternative sustainable and cost effective activators should be explored.

Regarding to ground granulated blastfurnace slag (GGBS), calcium hydroxide [$Ca(OH)_2$] and calcium oxide (CaO) have been reported to be potential activators because they are easily obtained and are much less expensive than sodium hydroxide or sodium silicate [9,11]. Slag concrete activated with $Ca(OH)_2$, with different auxiliary activators (Na_2SO_4 and Na_2CO_3), performed enhanced workability, delayed setting time and a similar increasing rate of compressive strength to PC concrete [12]. The comparison between the effect of CaO and $Ca(OH)_2$ in activating slag revealed that the use of CaO demonstrated a superior potential for the activation of GGBS and produced a higher mechanical strength than $Ca(OH)_2$ [11].

More recently, studies have indicated that reactive magnesia (MgO) could also serve as an effective activator for GGBS, showing its advantages in mechanical performances and the controllable setting time (which depends on the reactivity of MgO) [13–18]. The results by Yi et al. [17] showed that the reactive MgO activated GGBS achieved higher 28-day compressive strength than that of the corresponding $Ca(OH)_2$-GGBS system due to the larger content of the voluminous hydrotalcite-like phases having formed during the hydration. A later study proved that although reactive MgO-GGBS blends showed a lower slag hydration degree, they had better pore filling effect which resulted in higher 90-day strengths than the corresponding $Ca(OH)_2$-GGBS blends [18]. However, the early age strength of reactive MgO-GGBS blends was also found to be too low when the MgO content was <10-15wt% [18]. Although enhanced early strengths were observed by using MgO of higher reactivity [16], the cost becomes a concern. The current global production of MgO is ~20 million tonnes per year (~80% of which is produced in China, mainly from magnesite mines and the rest is produced from brines and seawater) [18] and the price of MgO with potential in slag activation varies from US$180 per ton to US$350 per ton in China

[19], which is lower than, for instance, NaOH (~US$500 per ton in China). Nevertheless, the cost of MgO usage needs further reduction. The study on the effect of different MgOs on the activation efficiency of GGBS by Jin et al. [16] showed that the reactive MgO containing the highest content of internal CaO produced higher UCS values, which was attributed to their higher pH of the pore solution and higher slag hydration degrees compared to those relatively purer MgOs. In this context, the mixture of MgO-CaO is worthy of investigating as a economically and technically feasible activator for GGBS because CaO is cheap (~US$70 per ton in China) . As a natural mixture of MgO-CaO, calcined dolomite has already been reported to be an effective activator to slag [20].

In the present study, seven MgO-CaO mixtures were used to activate slag in order to explore the influence of MgO/CaO ratio on the mechanical and hydration properties of slag pastes. The strength and the hydration degree of slag were examined by the unconfined compressive strength (UCS), pH of pore water and a selective dissolution method. The hydration products and the microstructural characteristics of MgO-CaO activated GGBS were thoroughly studied by thermogravimetric analysis (TGA), X-ray diffraction (XRD) and scanning electron microscope (SEM) imaging combined with energy-dispersive X-ray (EDX) analysis. Meanwhile, the influence of water to binder ratio (0.35, 0.38) and curing conditions of the paste samples (water cured and humidity cured) were also presented.

2. Materials and experimental procedures

2.1. Materials

The commercial materials used in this research included reactive MgO (grade 92/200 from Richard Baker Harrison, UK), CaO (from Tarmac and Buxton Lime and Cement, UK), and GGBS

(from Hanson, UK). The chemical compositions and physical properties for these materials are given in Table 1. The reactivity of the reactive MgO is ~100 s determined by the acetic acid test according to Shand [21] and is categorised as a medium reactive MgO [18].

2.2. Sample preparation

In the blends, the total amount of the activator (including MgO and/or CaO) was kept constant at 10% by weight. Seven mix formulations, as shown in Table 2, were prepared by changing the proportion of MgO and CaO, at water to binder ratios of 0.35 and 0.38. The nomenclature used for the samples was a combination referring to the contents of MgO and CaO in the mixes. For instance, M2.5C7.5 refers to the samples of 2.5% MgO and 7.5% CaO. Materials were fully mixed in dry form and then a pre-determined amount of water was added. After homogeneously mixed in a mixer, samples were casted into 40mm×40mm×40mm cubes covered with cling film and cured at 20°C. After 24h, samples were demoulded and cured under two different conditions: (1) immersed in deionised water and (2) sealed in plastic boxes at relative humidity of 99±1%. For both conditions, the curing temperature was kept constant at 20±1°C.

2.3. Experimental procedures

UCS measurements, using a constant load rate of 2400 N/sec, were undertaken in triplicate paste samples after curing for 7, 28 and 90 days. After the compression tests, the fractured paste samples were ground below 425 μm and then 10 g sample was weighted to mix with deionised water at a liquid to solid ratio of 1 ml/g in airtight containers according to [22]. The readings were taken in duplicate after 24 hours using a pH meter (Eutech 520) with an accuracy of ±0.01. Hydration of fractured paste samples were arrested by immersion in excess acetone for 3 days followed by vacuum dried for at least 3 days and oven dried for 1 day at 35°C. After drying, the

fractured pastes were gold coated for SEM/EDS analysis and also finely ground below 75 μm for XRD, TGA and selective dissolution tests. SEM/EDS were performed on JEOL 5800 and approximately 10 points on the gel were picked for the determination of elemental composition. Siemens D5000 X-ray diffractometer was used to collect XRD data with a scanning range between 5° and 55° 2θ. The scanning speed of 1 s/step and resolution of 0.05°/step were applied. Samples for TGA were heated from 40°C to 1000°C in air with the rate of heating at 10°C/min on a Perkin Elmer STA 6000 machine. The hydration degree of slag was determined by a selective dissolution method using salicyclic acid/methanol/acetone in duplicate according to Luke and Glasser [23]. This method is preferable to ethylene diamine tetraacetic acid (EDTA)/triethanolamine/NaOH technique due to the formation of hydrotalcite-like phase [11,15,24].

3. Results and discussions

3.1. Strength development

The strength development of the pastes with varying MgO/CaO ratios is shown in Fig.1 for the two different curing conditions and the specified w/c ratios. Generally, the strength of samples cured under the high humidity conditions was observed to be smaller than those of the water cured samples regardless of the curing age.

After 7 days, water cured samples with 10% CaO content (M0C10) gained strength of ~25MPa. The maximum strength was achieved when the MgO/CaO ratio was 1 (M5C5) and then it decreased significantly by the increase of the MgO content. It should be noted that the M10C0 paste only gained ~8MPa strength after 7 days, but a small amount of CaO addition (M9.5C0.5) resulted in a remarkable strength increase (~16MPa). The strength development after 28 days was

similar to that at 7 days for pastes with ≤8.5% MgO while the strength for pastes with ≥9.5% MgO (M9.5C0.5 and M10C0) increased more sharply, achieving ~25MPa. Compared with that at 7 days, the difference between M9.5C0.5 and M10C0 pastes was much smaller, especially for samples under high humidity curing, showing approximately the same strength. After 90 days, the strength of pastes M9.5C0.5 and M10C0 increased more notably to 41.8MPa and 42.6MPa, respectively, while the strength gained by other samples were relatively moderate. It was found that the strength for paste M10C0 was ~10% higher than that of M0C10 after 90 days, which is consistent with [18], who observed that reactive MgO outperformed lime in the long-term when activating GGBS.

For the samples prepared with w/c of 0.38 (Fig.1b), the compressive strength was, on average, ~27.4%, ~16.8% and ~17.4%, respectively, smaller than the pastes with w/c of 0.35 after each age, but with a similar trend to the pastes with w/c of 0.35. It was found that the water to binder ratio showed greater influence on the strengths in the early age.

For both w/c ratios, it can be seen that a small CaO content (~0.5%) significantly increased the early strength of high MgO-containing samples while it did not have much of an effect on the long term strength (90 days) of the pastes (Fig.1). On the other hand, the strength of all the pastes which contained ≤5% MgO showed inconspicuous difference at different times.

3.2. pH evolution

Various research indicates that pH has a significant effect on the hydration process of activated slag systems and also the nature of the products generated [25–34]. Higher pH environments usually induce better slag activation and higher mechanical strength. In order to

effectively activate the hydration of slag, the pH should be ≥11.5 [30,31]. It was also reported that, on the other hand, pH values <12 would delay the activation process [35].

Fig.2 presents the pH variations of the pastes with w/c of 0.35. All pH values except for paste M10C0 at 7 days were observed to be ≥12. For paste M10C0, the relatively low pH, compared to other CaO containing pastes, resulted in a slow hydration process and hence much lower strength, especially at 7 days. By contrast, pastes containing CaO presented much higher pH between 12.0 and 12.3 in the early age. At 28 days, pH of pastes containing CaO increased to ~12.5 due to the equilibrium of $Ca(OH)_2$ in pore solution while that of paste M10C0 was still at a low level. At 90 days, the pH of the pastes with ≥1.5% CaO content maintained pH of ~12.5 due to the sufficient presence of CaO providing sufficient OH^- after hydration and the equilibrium between the hydration products and the pore solution still existing. By contrast, those with less CaO decreased to ~12.3 which was induced by the consumption of $Ca(OH)_2$ through the reaction with GGBS. The pH of paste M10C0 continued to increase at 90 days, indicating the latent hydration of MgO and the hysteretic releasing of OH^- into the pore water. It should be noted that, compared with paste M10C0, a small dosage of CaO in the blend (i.e. paste M9.5C0.5) was associated with greatly increased pH at 7 and 28 days. Therefore the hydration was significantly accelerated in such high MgO content pastes during these periods.

3.3. Hydration kinetics

3.3.1. Slag dissolution

The percentage of anhydrous slag after different hydration periods allows the calculation of the fraction of slag reacted. Fig.3 presents the degrees of reacted slag of the water cured pastes with water to binder ratio of 0.35. An increase of MgO (and simultaneously a decrease of CaO)

content in the blends is observed to decrease the hydration degree (Fig.3) except for pastes M9.5C0.5 and M10C0 after 90 days, whose degree of hydration were observed to be boosted. Although the degree of reacted slag of pastes M10C0 and M9.5C0.5 were still lower than the other pastes, except for paste M8.5C1.5, they showed higher strengths than others which could be explained by the nature of the hydration products (as discussed later in Section 3.4). When the MgO/CaO ratio was ≤1, the samples showed only a moderate degree of hydration gain reaching values between 26.0% and 28.4% after 90 days, indicating that the hydration reaction was very fast during the early age but slowed down at later ages. The hydration process of paste M10C0 was very slow during the first 7 days (at 9.3%), but revealed high values ~21.0% after 90 days. Obviously, the presence of a little CaO induced a higher degree of reacted slag of paste M9.5C0.5 than M10C0 at each corresponding time.

3.3.2. Chemically bound water content

The chemically bound water content obtained by measuring the weight loss up to 650°C using TGA could be used as a measure of the hydration kinetics of blended cements [36–38]. To eliminate the influence of decomposition of calcite, weight loss up to 550°C was measured here although this may underestimate the amount of chemically bound water from slag hydration than was really happening since some portlandite may be consumed by carbonation during curing. The weight loss after 550°C was mainly attributed to the decomposition of calcite. Nevertheless, according to the weight losses given in Fig.4, the hydration gradually slowed down with the increasing content of MgO in the paste in the early age. After 28 days and longer, however, the water loss of different pastes showed smaller differences. For those with MgO content higher than

9.5%, sharp increases in weight loss were observed with hydration time and the bound water content were not necessarily smaller than others pastes after 28 days and longer.

The development trend in bound water content were slightly different from that in the degree of reacted slag (Fig.3). For instance, although the degree of reacted slag of M10C0 after 90 days was smaller than M0C10, their bound water contents were very close. It was attributed to the higher amount of hydrotalcite-like phases (discussed below) increased the bound water content of high MgO content pastes as the hydrotalcite-like phases ($Mg_4Al_2O_7{\cdot}10H_2O$) contains relatively more water than C-S-H [39].

3.4. Hydrates

3.4.1. X-ray diffraction

Fig.5 presents the X-ray diffraction patterns of pastes hydrated for 28 days in water. As the main hydration products of alkali-activated slag, C-S-H and hydrotalcite-like phases, can be clearly identified in all pastes agreeing with the literature [11,31,34,37,40]. Due to their semi-amorphous nature, the major peaks of C-S-H appeared with the background hump in the 2θ range of 25° to 35°. Hydrotalcite-like phases are common hydration products in alkali-activated GGBS when there is sufficient MgO content in the GGBS composition [41–44], hence it is not surprising to observe hydrotalcite-like phases in GGBS pastes activated by reactive MgO associated with CaO.

In high CaO content pastes (i.e. M0C10 and M5C5), the strong peaks corresponding to portlandite are detected, which can be attributed to the excess CaO added. On the other hand, the peaks of portlandite were not detected in the microgram of M9.5C0.5 and M10C0 (samples with

low content of CaO) due to its complete consumption in forming C-S-H and hydrotalcite-like phases after 28 days. The presence of calcite in M0C10 and M5C5 could have originated from the raw CaO and/or the carbonation of the formed portlandite. Unhydrated MgO phase observed around 43°2θ indicates the surplus supply of MgO for activating the slag in pastes M9.5C0.5 and M10C0. MgO present in cementitious system is predicted to precipitate initially as brucite [45]. However, brucite was not detected here, in agreement with the previous studies [17,18]. It may have converted to hydrotalcite-like phases although the formation of brucite was not confirmed when the XRD test performed.

3.4.2. Thermogravimetric analysis (TGA)

The TG/DTG curves of samples after 28 days hydration are given in Fig.6. At up to 300°C, the weight loss mainly corresponding to the thermal decomposition of C-S-H, according to [11,17,34,38,46], were observed in all pastes. The small shoulders around 80°C present the decomposition of ettringite [47,48], which originates from the sulphate content in the raw GGBS and CaO. However, this minor hydration product was not identified in the XRD result, probably due to its small content. The decomposition of the hydrotalcite-like phases induced a tiny shoulder at ~200°C and the weight loss between 330°C and 400°C, as reported by other researchers [38,48,49]. For pastes of high CaO content (i.e. M0C10 and M5C5), the dehydroxylation of portlandite can be observed at ~440°C. Beyond 600°C, considerable amount of $-CO_3^{2-}$ containing phases (mainly calcite) are observed, agreeing well with the XRD result.

To quantitatively analyse the amounts of the two hydration products (i.e. C-S-H and portlandite) after different hydration time, the weight losses between 40°C to 300°C and 400°C and 500°C can be calculated separately. Here define the weight loss of C-S-H in the former range as

Δm1 and that of portlandite between 400°C and 500°C as Δm2. Although the decomposition of other phases (ettringite, hydrotalcite-like phases) overlaps with C-S-H within this range, their influence is supposed to be small due to their relatively small amounts. In addition, the decomposition temperature of hydrotalcite-like phases overlaps with that of portlandite, therefore Δm2 was over estimated to some extent especially for pastes with high MgO content. The variations of Δm1 and Δm2 of samples over hydration time are summarised in Fig.7. Fig.7a reveals that the weight loss of C-S-H accounted for approximately 4.9% of the ignited weight in paste M0C10 and it gradually dropped to ~2.6% of that in paste M10C0 in the early age. It can be explained by the increased hydration rate which was in positive correlation with the content of CaO. Δm1 increased with the curing time due to the increased hydration degree as suggested by Fig.3 and the increments of paste M9.5C0.5 and M10C0 were relatively greater. After 28 days, the weight loss of these two pastes were close to, although still smaller, other samples (CaO wt.%≥ 2.5%) but almost at the same level by 90 days.

In general, Δm2 showed a negative relationship with MgO content and a positive relationship with time (Fig.7b). It is not surprising because the hydration of CaO produces portlandite therefore more CaO resulted in more portlandite. On the other hand, since no apparent characteristic peaks of portlandite were detected in XRD curves of M9.5C0.5 and M10C0 (Fig.5), Δm2 of these two samples after 28 days and 90 days can be attributed to the decomposition of hydrotalcite-like phases whose weight loss also appears around 400°C [17,34,38]. In this context, it can be concluded that more hydrotalcite-like phases formed in pastes with MgO content higher than 9.5% after 28 days and longer, therefore made significant contribution to the strength by its better pore filling effect.

3.4.3. Scanning electron microscopy

Fig.8 shows the SEM images of microstructure of selected paste samples after 28 days hydration. Dense C-S-H gels can be observed in all samples. The formation of plates of portlandite in Fig.8a and apparent presence of platelet hydrotalcite-like phases in Fig.8b and c agree well with the analyses by XRD and TGA (Fig.5 and Fig.6).

Fig.9b shows a much denser M9.5C0.5 microstructure of 90 days that that of 28 days (Fig.9a) in a different scale bar. It may be attributed to (i) more C-S-H formed after longer hydration according to Fig.7a and (ii) the significantly pore filling effect hydrotalcite-like phases, which are more voluminous than C-S-H. That more hydrotalcite-like phases formed in pastes in high MgO content was confirmed by TG analysis (see Section 3.4.2).

3.4.4. Energy-dispersive X-ray microanalysis

Combined with SEM, EDS analysis was conducted to determine the differences in the elemental composition of the hydrate phases. The Ca/Si and Mg/Al ratios calculated from chemical compositions of the anhydrous binders (see Table 1) are summarised in Table 3. These initial ratios varied due to the different dosages of added MgO and CaO. The average ratios obtained from EDS analysis are also given in Table 3.

For alkali-activated slag, previous research suggested that the Ca/Si ratio of C-S-H gel ranges from 0.6 to 2.3, depending on the type of activator, the curing condition and the nature of the slag [30,34,42,43,50]. Table 3 shows that after 28 days, the Ca/Si ratio of the gel decreased from 1.59 for M0C10 to 1.45 for M10C0, in agreement with the initial Ca/Si ratio, which decreased from 1.46 to 1.16 when the CaO content decreased from 10% to 0%. Pastes with a higher pH (>11.5)

pore solution were reported to have a lower Ca/Si ratio due to the fact that the solubility of Si increased with pH while that of Ca decreased [30,31]; the slight increase of Ca/Si ratio with the increase of CaO content is attributed to the increased Ca^{2+} ion availability and hence higher uptake of Ca^{2+} ion in C-S-H gel.

The Mg/Si versus Al/Si ratios are plotted in Fig.10 for all hydration periods together. The linear slope confirms the presence of hydrotalcite-like phases with Mg/Al ratio from 1.32 for paste M0C10 to 1.93 for paste M10C0, which are higher than the initial Mg/Al ratios given in Table 3. Increasing the MgO content resulted in a higher Mg/Al ratio of the hydration products due to the increased availability of Mg ions for reaction. In addition, the intercept bigger than 0.2 in the Al/Si axis suggests that the C-S-H gel contains significant proportions of aluminium, agreeing well with others [18,24].

4. Conclusions

Ground granulated blastfurnace slag was activated using reactive MgO, CaO, and MgO-CaO mixtures and their mechanical and hydration properties were studied. Based on the experimental results, the following conclusions can be drawn:

(1) The performance of slag pastes activated with MgO-CaO mixtures depended on the ratio of MgO to CaO. The strength of slag pastes decreased with the increasing ratio of MgO to CaO in the early age while a much steeper strength gain was observed in pastes with MgO to CaO ratio higher than 19/1 (i.e. M9.5C0.5 and M10C0) after 28 days and longer. Pastes showed small difference in strength development at each period when the ratio of MgO to CaO was less than 1.

(2) The addition of CaO in MgO can increase the pH of the pore solution, and hence significantly accelerate the activation of slag in the early age. In this study, 0.5% CaO blended

with 9.5% MgO was found to notably increase the early strength of the paste.

(3) The hydration degree of slag decreased with the increasing MgO/CaO ratio, but this trend was not applicable for pastes with MgO/CaO ratios higher than 19/1 after 90 days due to the delayed activation of the slag by MgO.

(4) XRD and TGA results showed that the hydration products of activated slag using MgO-CaO mixtures were mainly C-S-H and hydrotalcie-like phases. Portlandite and calcite were also observed and their quantities depended on the MgO/CaO ratio. The amount of C-S-H was found to be in positive correlation to the content of CaO in slag in the early age while more hydrotalcite-like phases formed in high MgO content pastes after 28 days and longer.

(5) By increasing the MgO/CaO ratio in the mixture, the average Ca/Si ratio of C-S-H gels after 28 days decreased from 1.59 to 1.45. The Mg/Al ratio for the hydrotalcite-like phases varied from 1.3 to 1.9, depending on the MgO/CaO ratio.

(6) For MgO-CaO-GGBS system, higher compressive strengths of pastes can be achieved by lower w/c ratio and using water curing instead of humidity curing.

Acknowledgements

The work presented in this paper was carried out at Department of Engineering, University of Cambridge, where the first author was a visiting researcher. The visit was funded by the China Scholarship Council and the Scientific Research Foundation of the Graduate School of Nanjing University (No.2012CL11). The financial support for the PhD studentship of the second author from the Cambridge Trust and China Scholarship Council was also very much appreciated.

References

[1] Provis JL, van Deventer JSJ. Alkali Activated Materials:State-of-the-Art Report, RILEM TC 224-AAM. Dordrecht: Springer Netherlands; 2014.

[2] Shi C, Jiménez AF, Palomo A. New cements for the 21st century: The pursuit of an alternative to Portland cement. Cem Concr Res 2011;41:750–63.

[3] Provis JL. Geopolymers and other alkali activated materials: why, how, and what? Mater Struct 2013;47:11–25.

[4] Rashad AM. A comprehensive overview about the influence of different additives on the properties of alkali-activated slag – A guide for Civil Engineer. Constr Build Mater 2013;47:29–55.

[5] Habert G, d'Espinose de Lacaillerie JB, Roussel N. An environmental evaluation of geopolymer based concrete production: reviewing current research trends. J Clean Prod 2011;19:1229–38.

[6] Duxson P, Provis JL, Lukey GC, van Deventer JSJ. The role of inorganic polymer technology in the development of "green concrete." Cem Concr Res 2007;37:1590–7.

[7] Turner LK, Collins FG. Carbon dioxide equivalent (CO2-e) emissions: A comparison between geopolymer and OPC cement concrete. Constr Build Mater 2013;43:125–30.

[8] Yang K-H, Song J-K, Ashour AF, Lee E-T. Properties of cementless mortars activated by sodium silicate. Constr Build Mater 2008;22:1981–9.

[9] Yang K-H, Cho A-R, Song J-K, Nam S-H. Hydration products and strength development of calcium hydroxide-based alkali-activated slag mortars. Constr Build Mater 2012;29:410–9.

[10] Van Deventer JSJ, Provis JL, Duxson P. Technical and commercial progress in the adoption of geopolymer cement. Miner Eng 2012;29:89–104.

[11] Kim MS, Jun Y, Lee C, Oh JE. Use of CaO as an activator for producing a price-competitive non-cement structural binder using ground granulated blast furnace slag. Cem Concr Res 2013;54:208–14.

[12] Yang K-H, Cho A-R, Song J-K. Effect of water–binder ratio on the mechanical properties of calcium hydroxide-based alkali-activated slag concrete. Constr Build Mater 2012;29:504–11.

[13] Shen W, Wang Y, Zhang T, Zhou M, Li J, Cui X. Magnesia modification of alkali-activated slag fly ash cement. J Wuhan Univ Technol Sci Ed 2011;26:121–5.

[14] Li X. Mechanical properties and durability performance of reactive magnesium cement concrete, PhD thesis. University of Cambridge, UK, 2012.

[15] Jin F, Abdollahzadeh A, Al-Tabbaa A. Effect of different MgO on the hydration of MgO-activated granulated ground blastfurnace slag paste. Proc. Int. Conf. Sustain. Constr. Mater. Technol., Kyoto, Japan: 2013.

[16] Jin F, Gu K, Abdollahzadeh A, Al-Tabbaa A. Effect of different reactive MgOs on the hydration of MgO-activated ground granulated blastfurnace slag paste. J Mater Civ Eng 2014:doi:10.1061/(ASCE)MT.1943–5533.0001009.

[17] Yi Y, Liska M, Al-Tabbaa A. Properties and microstructure of GGBS–magnesia pastes. Adv Cem Res 2013:1–9.

[18] Jin F. Characterisation and Performance of reactive MgO-based cements, PhD thesis. University of Cambridge,UK, 2014.

[19] Beijing HL Consulting Company. Market research report on magnesia(MgO)industry in China 2009. 2009.

[20] Gu K, Jin F, Al-Tabbaa A, Shi B. Activation of ground granulated blast furnace slag by using calcined dolomite. Constr Build Mater 2014:doi:10.1016/j.conbuildmat.2014.06.044.

[21] Shand MA. The chemistry and technology of magnesia. Hoboken,New Jersey: John Wiley & Sons; 2006.

[22] Hidalgo A, Garcia JL, Aloson MC, Fernandez-Luco L, Andrade C. Testing methodology for pH determination of cementitious materials. application to low pH binders for use in HLNWR. In: Bäckblom G, editor. 2nd Work. R&D low-pH Cem. a Geol. Repos., Madrid: 2005.

[23] Luke K, Glasser F. Selective dissolution of hydrated blast furnace slag cements. Cem Concr Res 1987;17:273–82.

[24] Ben Haha M, Lothenbach B, Le Saout G, Winnefeld F. Influence of slag chemistry on the hydration of alkali-activated blast-furnace slag — Part II: Effect of Al2O3. Cem Concr Res 2012;42:74–83.

[25] Roy A, Schilling PJ, Eaton HC, Malone PG, Brabston WN, Wakeley LD. Activation of Ground Blast-Furnace Slag by Alkali-Metal and Alkaline-Earth Hydroxides. J Am Ceram Soc 1992;75:3233–40.

[26] Wang S, Scrivener K, Pratt P. Factors affecting the strength of alkali-activated slag. Cem Concr Res 1994;24:1033–43.

[27] Wang S-D, Scrivener KL. Hydration products of alkali activated slag cement. Cem Concr Res 1995;25:561–71.

[28] Shi C, Day R. Some factors affecting early hydration of alkali-slag cements. Cem Concr Res 1996;26:439–41.

[29] Bakharev T, Sanjayan JG, Cheng Y-B. Alkali activation of Australian slag cements. Cem Concr Res 1999;29:113–20.

[30] Song S, Jennings H. Pore solution chemistry of alkali-activated ground granulated blast-furnace slag. Cem Concr Res 1999;29:159–70.

[31] Song S, Sohn D, Jennings H, Mason T. Hydration of alkali-activated ground granulated blast furnace slag. J Mater Sci 2000;35:249–57.

[32] Li Y, Sun Y. Preliminary study on combined-alkali–slag paste materials. Cem Concr Res 2000;30:963–6.

[33] Oh JE, Monteiro PJM, Jun SS, Choi S, Clark SM. The evolution of strength and crystalline phases for alkali-activated ground blast furnace slag and fly ash-based geopolymers. Cem Concr Res 2010;40:189–96.

[34] Ben Haha M, Le Saout G, Winnefeld F, Lothenbach B. Influence of activator type on hydration kinetics, hydrate assemblage and microstructural development of alkali activated blast-furnace slags. Cem Concr Res 2011;41:301–10.

[35] Fernández-Jiménez A, Puertas F. Effect of activator mix on the hydration and strength behaviour of alkali-activated slag cements. Adv Cem Res 2003;15:129–36.

[36] Bhatty J. A review of the application of thermal analysis to cement-admixture systems. Thermochim Acta 1991;189:313–50.

[37] Escalante-García JI, Fuentes AF, Gorokhovsky A, Fraire-Luna PE, Mendoza-Suarez G. Hydration Products and Reactivity of Blast-Furnace Slag Activated by Various Alkalis. J Am Ceram Soc 2003;86:2148–53.

[38] Gruskovnjak A, Lothenbach B, Winnefeld F, Münch B, Figi R, Ko S-C, et al. Quantification of hydration phases in supersulfated cements: review and new approaches. Adv Cem Res 2011;23:265–75.

[39] Ben Haha M, Lothenbach B, Le Saout G, Winnefeld F. Influence of slag chemistry on the hydration of alkali-activated blast-furnace slag — Part I: Effect of MgO. Cem Concr Res 2011;41:955–63.

[40] Puertas F, Martínez-Ramírez S. Alkali-activated fly ash/slag cements: strength behaviour and hydration products. Cem Concr Res 2000;30:1625–32.

[41] Brough AR, Atkinson A. Sodium silicate-based , alkali-activated slag mortars Part I . Strength , hydration and microstructure 2002;32:865–79.

[42] Richardson J, Biernacki J. Stoichiometry of slag hydration with calcium hydroxide. J Am Ceram Soc 2002;85:947–53.

[43] Richardson I, Brough A, Groves G, Dobson C. The characterization of hardened alkali-activated blast-furnace slag pastes and the nature of the calcium silicate hydrate (CSH) phase. Cem Concr Res 1994;24:813–29.

[44] Le Saoût G, Ben Haha M, Winnefeld F, Lothenbach B. Hydration Degree of Alkali-Activated Slags: A 29Si NMR Study. J Am Ceram Soc 2011;94:4541–7.

[45] Lothenbach B, Winnefeld F. Thermodynamic modelling of the hydration of Portland cement. Cem Concr Res 2006;36:209–26.

[46] Michel M, Georgin J-F, Ambroise J, Péra J. The influence of gypsum ratio on the mechanical performance of slag cement accelerated by calcium sulfoaluminate cement. Constr Build Mater 2011;25:1298–304.

[47] Lothenbach B, Wieland E. A thermodynamic approach to the hydration of sulphate-resisting Portland cement. Waste Manag 2006;26:706–19.

[48] Gruskovnjak A, Lothenbach B, Winnefeld F, Figi R, Ko S-C, Adler M, et al. Hydration mechanisms of super sulphated slag cement. Cem Concr Res 2008;38:983–92.

[49] Parashar P, Sharma V, Agarwal DD, Richhariya N. Rapid synthesis of hydrotalcite with high antacid activity. Mater Lett 2012;74:93–5.

[50] Wang S-D, Scrivener KL. 29Si and 27Al NMR study of alkali-activated slag. Cem Concr Res 2003;33:769–74.

The list of captions for all tables:

1. **Table 1. Chemical compositions and physical properties of raw materials (from suppliers' datasheets)**
2. **Table 2. Mix compositions of the pastes**
3. **Table 3. Atomic ratios obtained by theoretical calculation and EDS analyses**

The list of captions for all figures:

1. **Fig.1 Compressive strength of the pastes at two different water/binder rations of (a) w/c=0.35 and (b) w/c=0.38.**
2. **Fig.2 pH variation of water cured pastes with time, w/c=0.35.**
3. **Fig.3 Variation of degree of reacted slag with MgO content, w/c=0.35.**
4. **Fig.4 Weight loss between 40°C and 550°C determined by TGA (weight percentage relative to the ignited samples), w/c=0.35.**
5. **Fig.5 XRD patterns of selected samples after 28 days.**
6. **Fig.6 TG/DTG curves of samples after a hydration time of 28 days.**
7. **Fig.7 Weight losses in two temperature ranges (a) Δm1 and (b) Δm2.**
8. **Fig.8 Representative SEM images of hydrated samples after 28 days showing the typical hydration products: A: C-S-H, B: portlandite, C: hydrotalcite-like phases for three different pastes at 28 days: (a) M0C10, (b) M9.5C0.5 and (c) M10C0.**
9. **Fig.9 SEM images of C0.5M9.5 after two different hydration periods. (a) 28 days, (b) 90 days.**
10. **Fig.10 Atomic ratios Mg/Si vs. Al/Si of the samples after 28 days.**

Table 1

Click here to download Table: Table 1.docx

Table 1. Chemical compositions and physical properties of raw materials (from suppliers' datasheets)

	GGBS	MgO	CaO
Chemical composition			
SiO_2	37.0	0.9	0.9
Al_2O_3	13.0	0.22	0.13
CaO	40.0	0.9	94.0
MgO	8.0	>93.2	0.5
K_2O	0.6	-	-
Na_2O	0.3	-	-
SO_3	1.0	-	0.06
Fe_2O_3	-	0.5	0.08
$CaCO_3$	-	-	3.7
Physical properties			
Specific surface area(m^2/g)	0.49	9.00	-
Bulk density (kg/m^3)	1050	-	1020

Table 2

Click here to download Table: Table 2.docx

Table 2. Mix compositions of the pastes

Sample	activator/ slag	MgO/ CaO	weight percentage(%)			water/binder
			MgO	CaO	GGBS	
M0C10	1/9	0/10	0	10	90	0.35 & 0.38
M2.5C7.5		1/3	2.5	7.5	90	0.35
M5C5		1/1	5	5	90	0.35 & 0.38
M7.5C2.5		3/1	7.5	2.5	90	0.35
M8.5C1.5		17/3	8.5	1.5	90	0.35 & 0.38
M9.5C0.5		19/1	9.5	0.5	90	0.35 & 0.38
M10C0		10/0	10	0	90	0.35 & 0.38

Table 3

Click here to download Table: Table 3.docx

Table 3. Atomic ratios obtained by theoretical calculation and EDS analyses

Sample	Age (days)	Ca/Si	Mg/Al
M0C10	initial	1.46	0.79
	28	1.59	-
M5C5	initial	1.31	1.29
	28	1.56	-
	90	1.54	-
M9.5C0.5	initial	1.17	1.75
	7	1.12	-
	28	1.57	-
	90	2.07	-
M10C0	initial	1.16	1.80
	28	1.45	-

Figure 1

Click here to download high resolution image

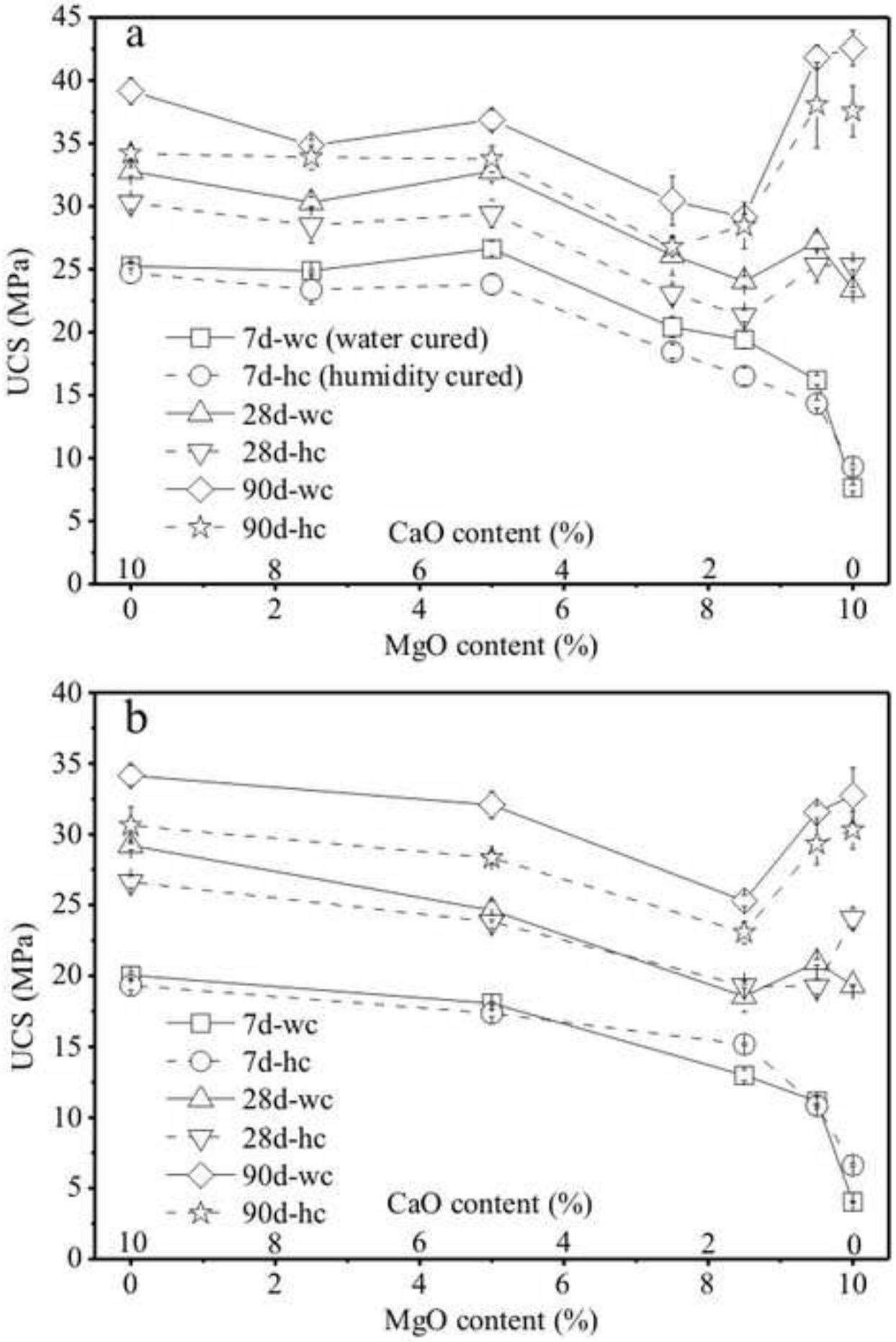

Figure 2

Click here to download high resolution image

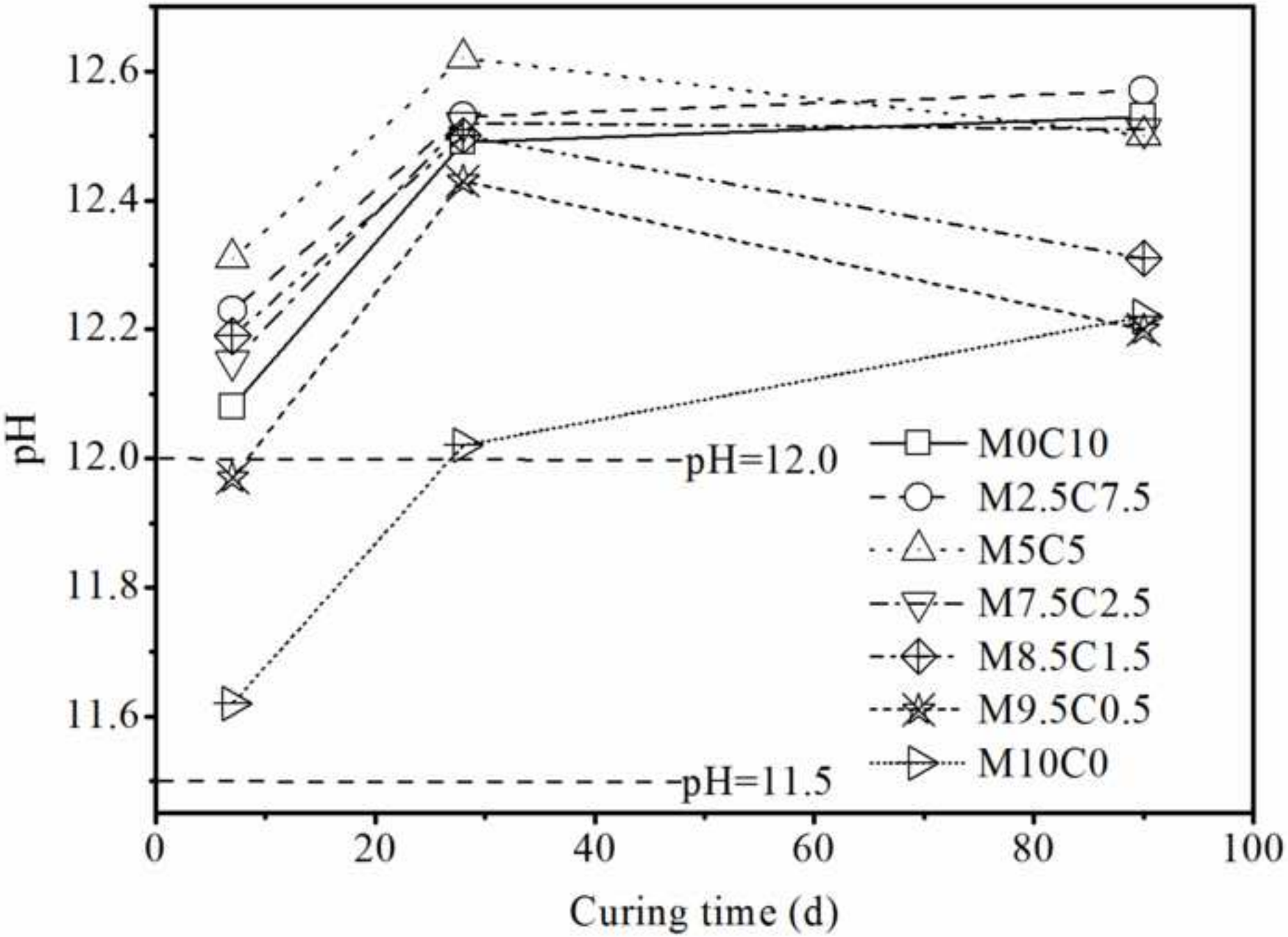

Figure 3

Click here to download high resolution image

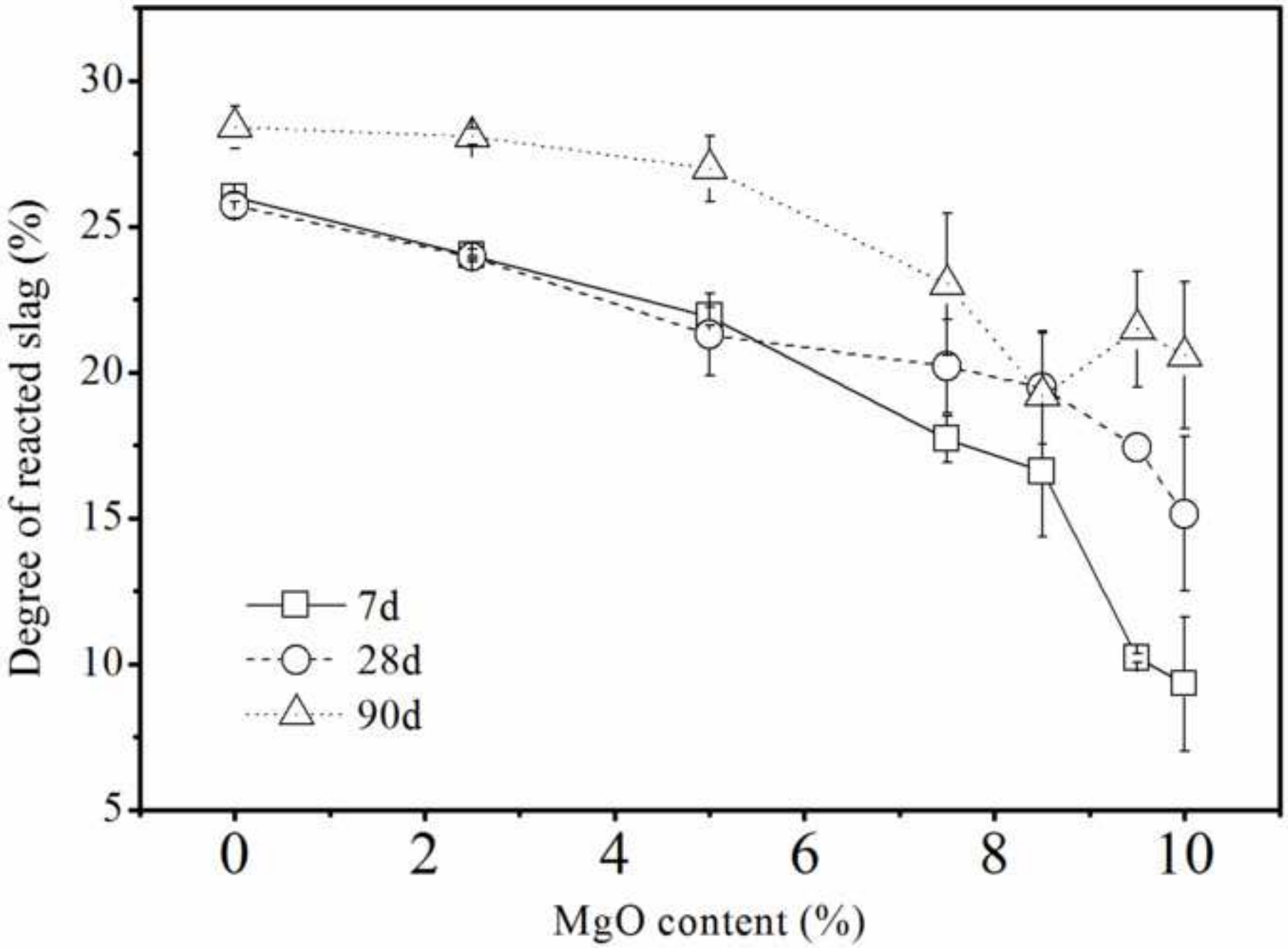

Figure 4

Click here to download high resolution image

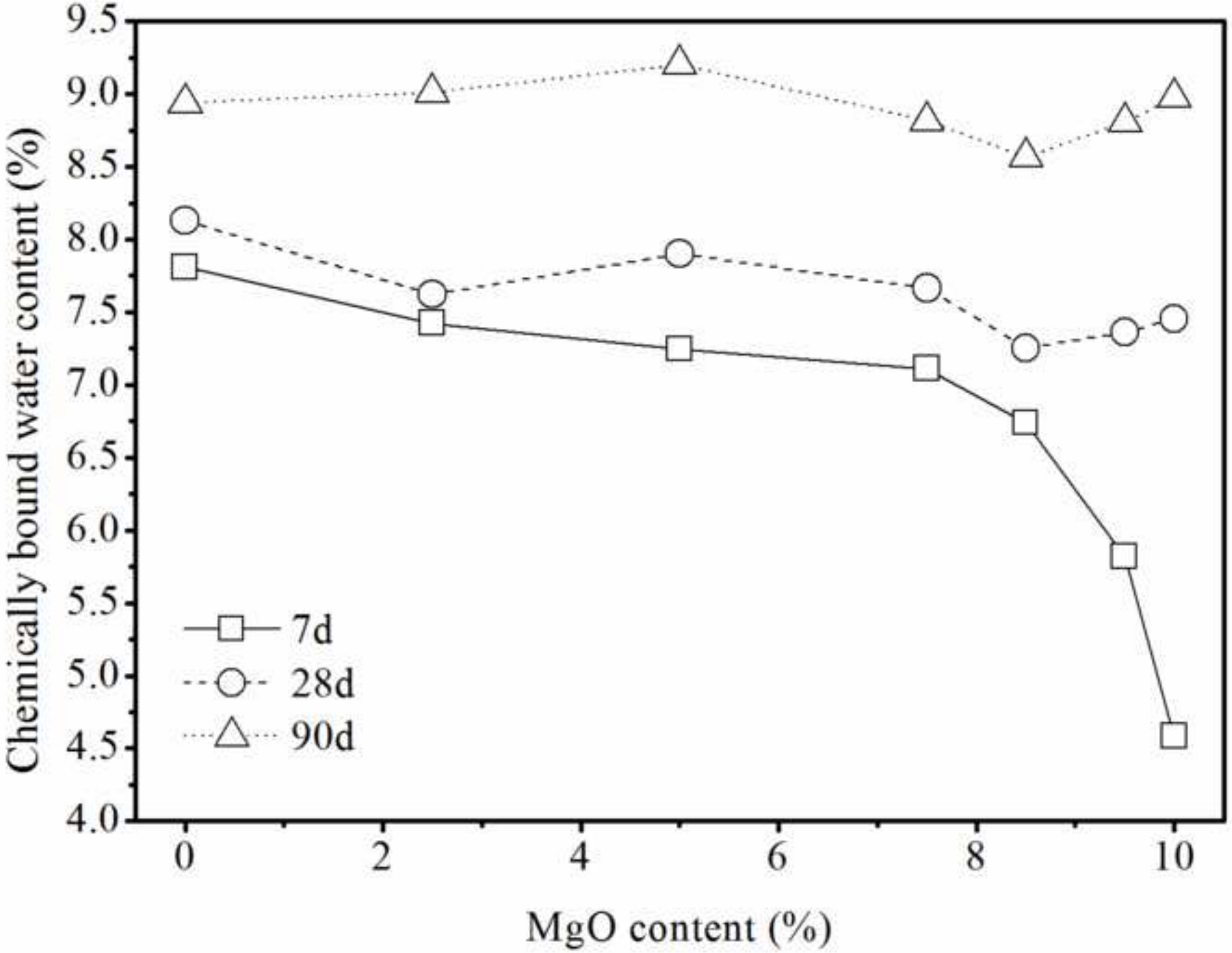

Figure 5

Click here to download high resolution image

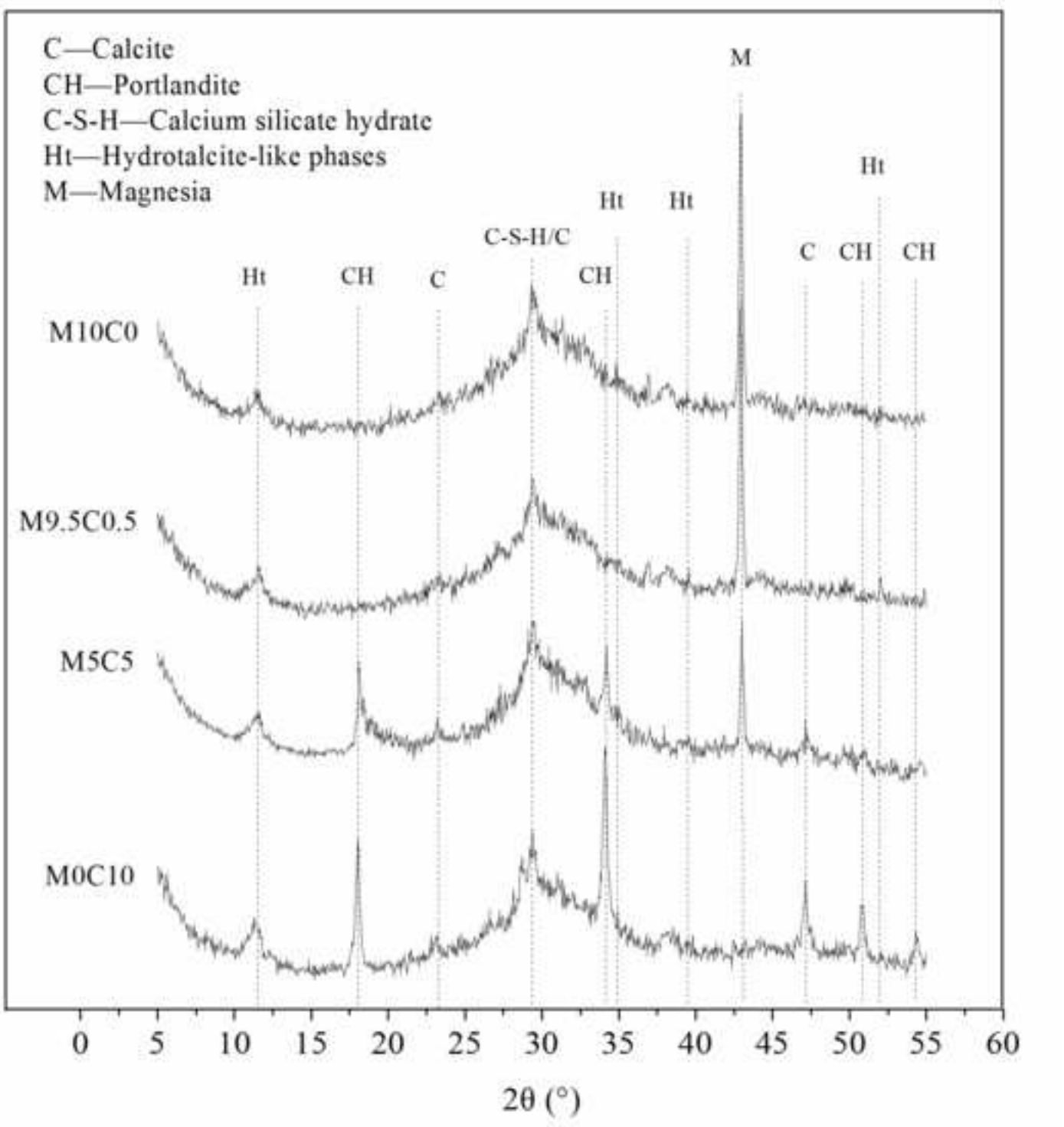

Figure 6

Click here to download high resolution image

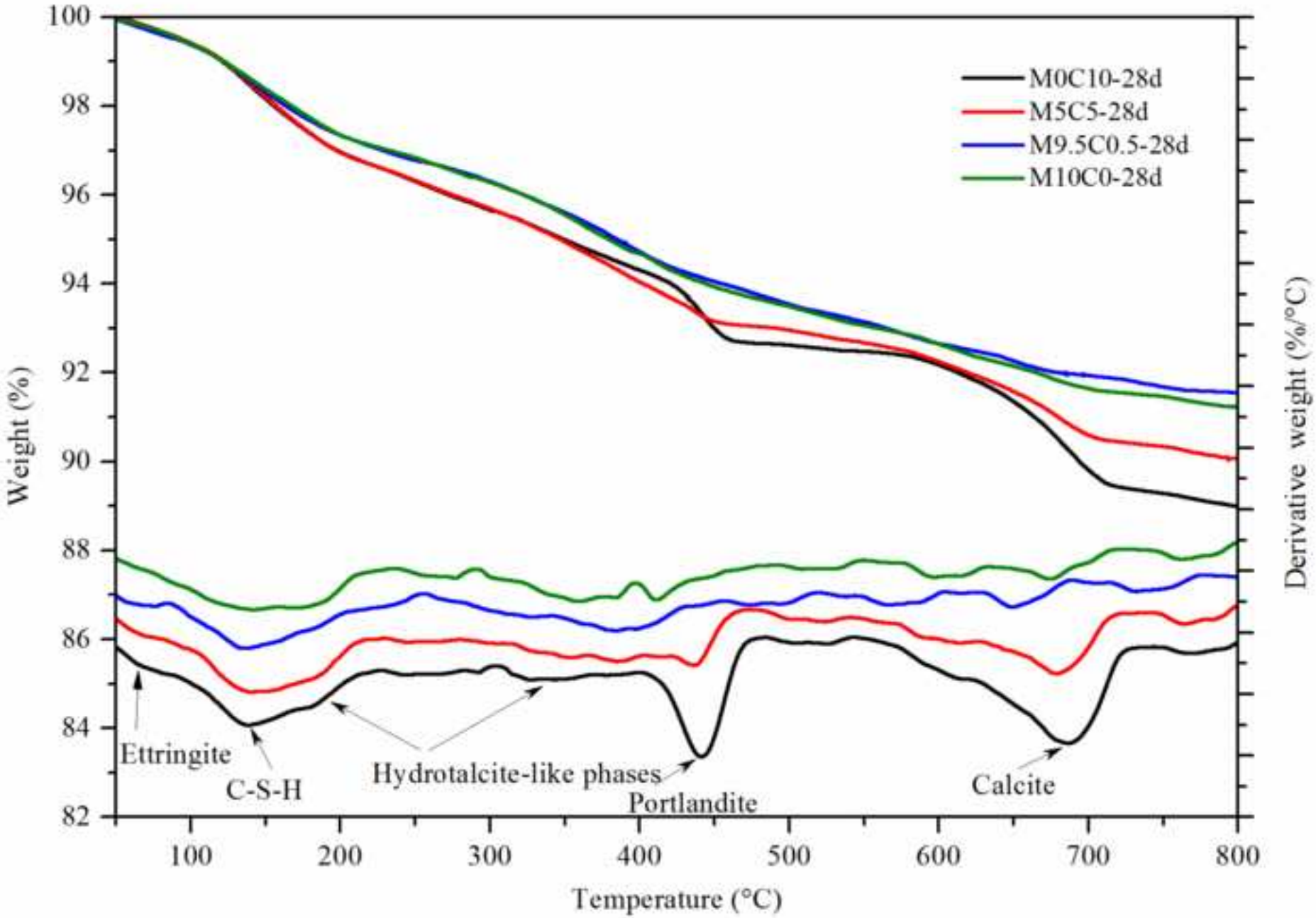

Figure 7

Click here to download high resolution image

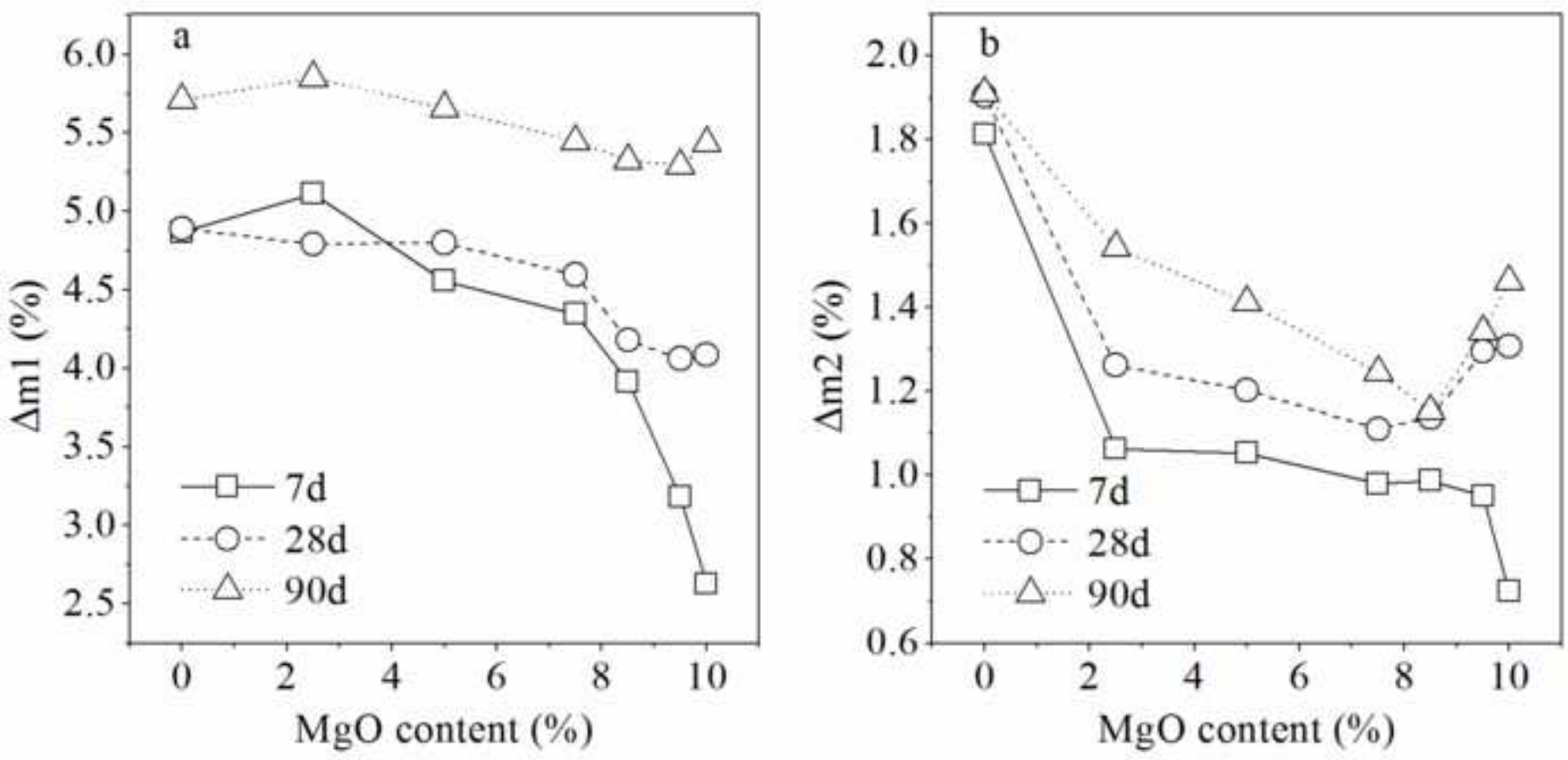

Figure 8

Click here to download high resolution image

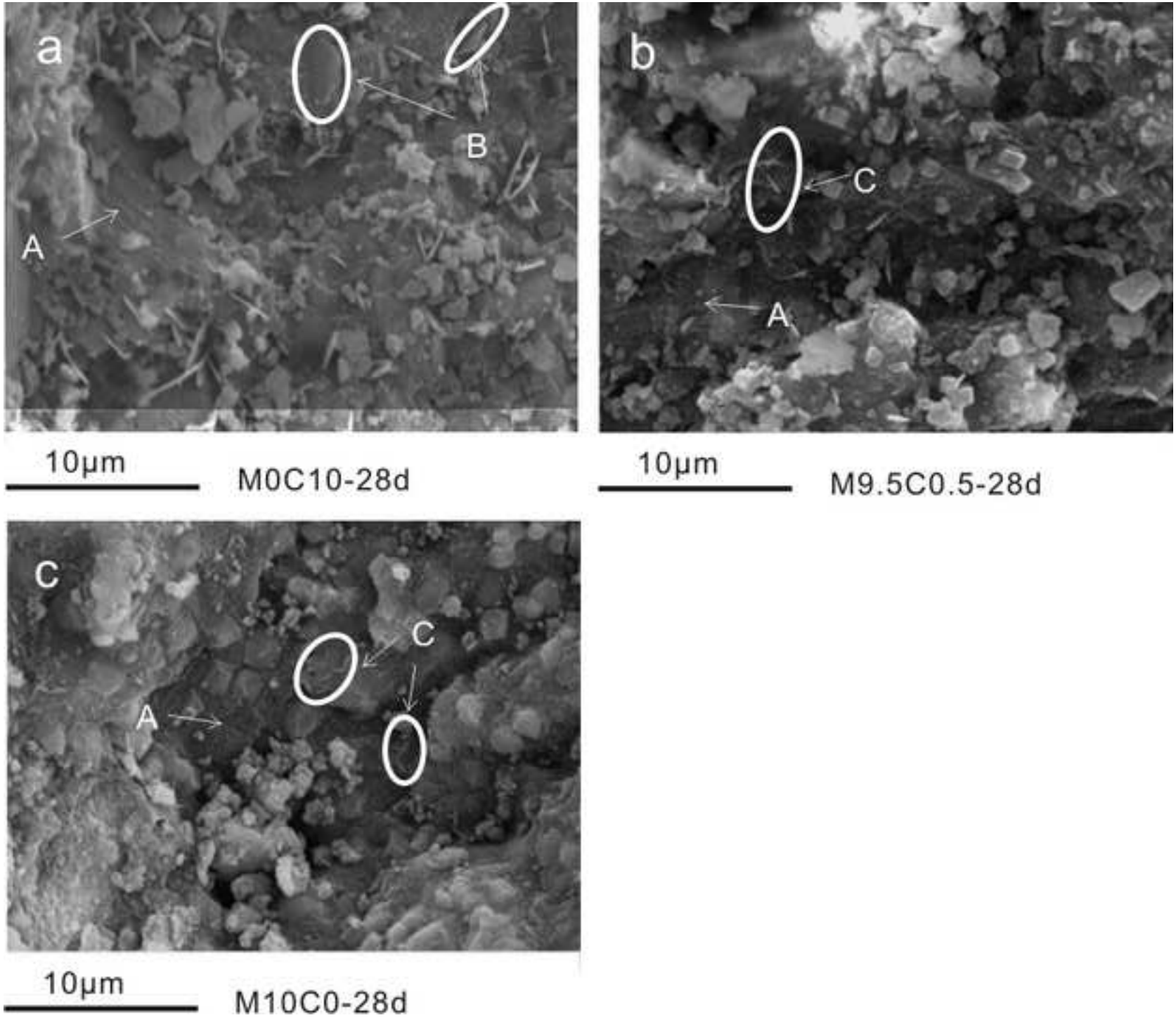

Figure 9
Click here to download high resolution image

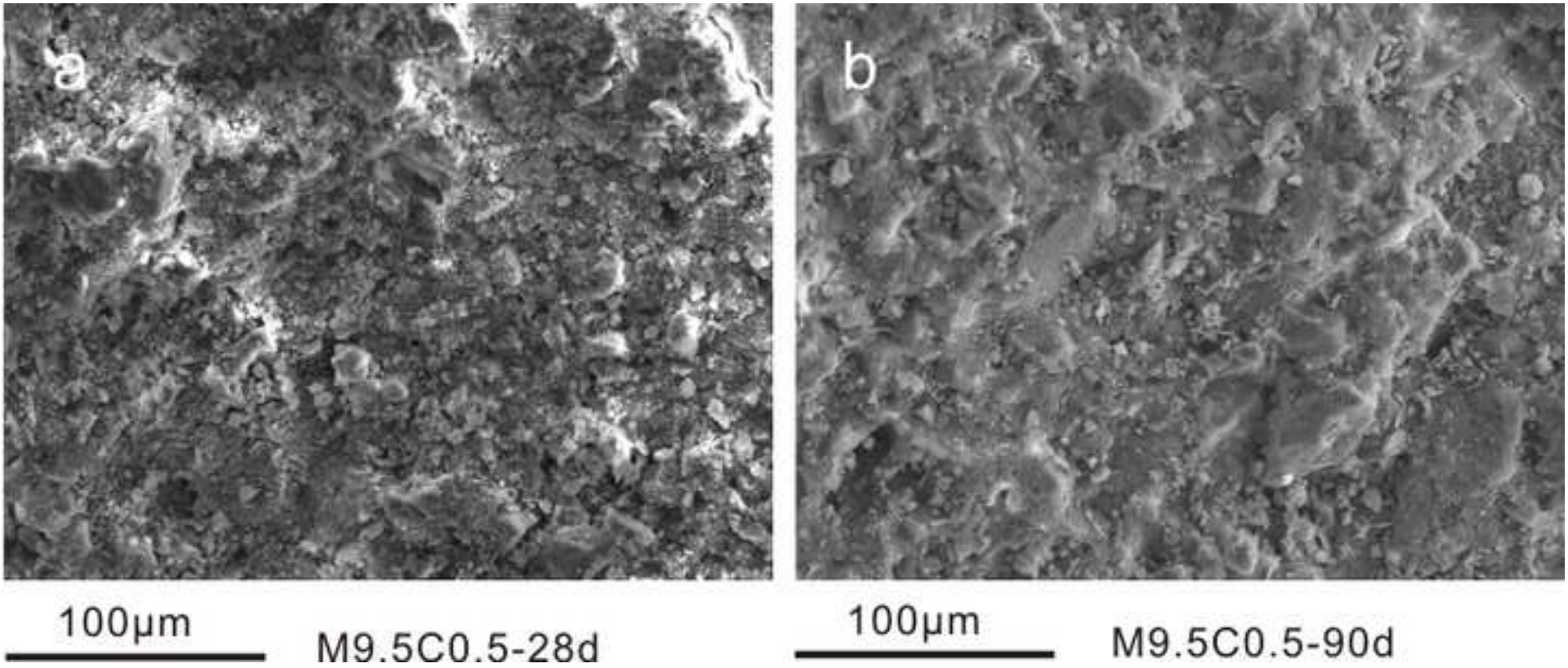

Figure 10

Click here to download high resolution image